Structural Properties of Post Annealed ITO Thin Films at Different Temperatures

Manavizadeh, Negin*[+]; Khodayari, Alireza; Asl Soleimani, Ebrahim; Bagherzadeh, Sheida

Thin Film Laboratory, ECE Department, University of Tehran, Tehran, I.R. IRAN

Maleki, Mohammad Hadi

Nuclear Science and Technology Research Institute, Laser and Optics Research School, Tehran, I.R. IRAN

ABSTRACT: *Indium tin oxide (ITO) thin films were deposited on glass substrates by RF sputtering using an ITO ceramic target (In_2O_3-SnO_2, 90-10 wt. %). After deposition, samples were annealed at different temperatures in vacuum furnace. The post vacuum annealing effects on the structural, optical and electrical properties of ITO films were investigated. Polycrystalline ITO films have been analyzed in wide optical spectrum, X-ray diffraction and four point probe methods. The results show that increasing the annealing temperature improves the crystallinity of the films. The resistivity of the deposited films is about 19×10^{-4} Ωcm and falls down to 7.3×10^{-5} Ωcm as the annealing temperature is increased to 500 °C in vacuum.*

KEY WORD: *RF sputtering, Indium tin oxide, Annealing in vacuum, Transparent conductive films.*

INTRODUCTION

In_2O_3 crystallizes to form the bixbyite structure (also called the C-type rare-earth oxide structure) [1]. The lattice constant is reported to be 1.0118 nm [2]. One unit cell consists of 16 units of In_2O_3. Therefore, for defect free In_2O_3, there are 80 atoms in one unit cell. Indium cations are located in two non-equivalent site which are shown in Fig. 1 [3], where 8 In^{3+} ions are located in the center of trigonally distorted oxygen octhahedrons (b site) and the remaining 24 In^{3+} ions are located in the center of the more distorted octahedrons (d site). Indium tin oxide is essentially formed by doping substitution of In_2O_3 with Sn which replaced the In^{3+} atoms from the cubic bixbyite structure of indium oxide. It was found that tin atoms preferentially occupy the less distorted b lattice sites in the expanded In_2O_3 lattice [4,5].

ITO films have high transmittance, high infrared reflectance, good electrical conductivity, excellent substrate adherence and hardness [6]. These layers are commonly used in various applications such as displays [7], sensors [8], solar cells [9], electro chromic devices [10], heatable [11], and so on. The most commonly used methods for ITO deposition are sputtering, thermal evaporation, spray pyrolysis, pulsed laser deposition (PLD) and screen printing technique and sol-gel [12-19]. To obtain high quality ITO films, usually these films are annealed after deposition.

Post-deposition annealing at temperatures above 200 °C is effective on grain growth or crystallinity of ITO thin films [20,21], resulting in reducing structural defects. Changes in the optical and electrical characteristics with

* *To whom correspondence should be addressed.*
+ *E-mail: manavizdeh@ee.kntu.ac.ir*
1021-9986/09/2/57 5/$/2.50

the annealing temperature have been associated with changes in the local ordering of the material during crystallization and also to oxygen-vacancy creation and/or annihilation that depends on the annealing atmosphere.

Annealing in an oxygen-deficient atmosphere not only promotes crystalline growth but also increases the carrier concentration by oxygen-vacancy creation [22]. The ITO samples obtained in Ar atmosphere or at oxygen deficiency are characterized by a sharp decrease in the resistivity. Another method of producing oxygen-vacancy is annealing in vacuum ambient [23].

To obtain high quality of ITO films, sol-gel is not a good technique due to perform in atmosphere ambient. As mentioned above, in this situation ITO layers have a few vacancies, so their resistivity will increase [24]. Comparing to thermal evaporation method [25], resistivities which are presented here, are lower.

We reported here a study of the structural, electrical and optical properties of ITO films deposited by RF sputtering using oxide target on glass substrates and annealed at different temperatures.

EXPERIMENTAL

ITO films were deposited utilizing RF sputtering in a load lock fitted vessel. The composition of 3 inch diameter oxide ceramic target (99.99 % purity) is 90 wt. % In_2O_3 and 10 wt. % SnO_2. Micro slide glass substrates (150 μm thickness) were cleaned by RCA method (DI water, ammonia, hydrogen peroxide 5:1:1).

The distance between the target and the substrates was 60 mm. The vacuum chamber was evacuated down to a base pressure of about 6×10^{-6} Torr prior to deposition. The reactive sputtering gas was high purity argon (99.999 %). The deposition was done at constant power of 280 W and pressure of 20 mTorr. All samples were deposited with same thickness of 400 nm.

During deposition, substrates are not externally heated but the temperature of the substrates due to ambient in plasma and relatively high power of deposition i.e. 280W, raises to about 120 °C. After the deposition, all the prepared samples in the same sputtering conditions were separately annealed in the vacuum furnace in pressure lower than 5×10^{-5} Torr for about 2h at temperatures 200, 300, 400 and 500 °C.

Film structure has been analyzed by X-ray diffraction (XRD Phillips) to investigate the present phases and to evaluate their degree of crystallinity. The resistivity of the film was calculated based on the resistance measured by a standard four-point probe technique (Keittley 196 & 224) at room temperature. The transmittances were measured in the spectral range from 200 to 2000 nm with UV/VIS/IR Spectrophotometer (Varian, Cary 500). The morphological property of the ITO layers was analyzed by scanning electron microscopy (SEM).

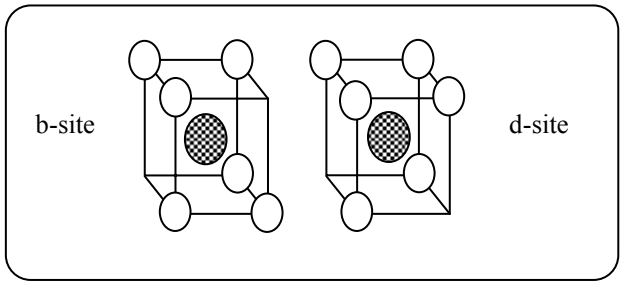

Fig. 1: Two non-equivalent sites of In atoms in In_2O_3 crystal [3].

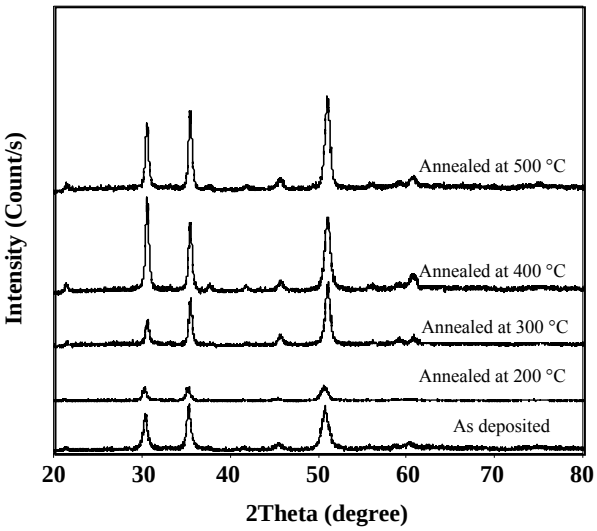

Fig. 2: XRD spectra of the ITO layers deposited at 280 W: as deposited and after annealing at 300 °C, 400 °C and 500 °C.

RESULTS AND DISCUSSION

After deposition at constant sputtering power of 280 W, samples were annealed in vacuum furnace at different temperatures. XRD patterns corresponding to the ITO thin films as grown by sputtering on micro slide glass substrates, as-deposited and in various annealing temperatures are shown in Fig. 2.

It is observed that all deposited ITO thin films are crystalline and have (222) and (400) preferred orientations even in case of asdeposited. All the peaks can be

Table 1: Parameters of ITO deposited utilizing RF sputtering and annealed in vacuum.

	Annealing temp. (°C)				
	As deposited	200	300	400	500
E_g (eV)	3.95	3.89	3.81	3.77	3.65
$\rho\times10^{-4}$ (Ωcm)	19.06	6.7	6.31	0.99≈1	0.73
I(222)/I(400)	0.8	1.03	0.42	1.94	0.85
Film texture	<100>	<111>	<100>	<111>	<100>
Lattice constant (Å)	10.154	10.013	10.102	10.101	10.063
$d_{(222)}$	2.933	2.945	2.905	2.916	2.905
$d_{(400)}$	2.538	2.526	2.523	2.514	2.530
T_{ave} (400-800nm) (%)	79.24	79.15	79.1	79	78.9

assigned to the cubic bixbyite structure of In_2O_3. In this research, after deposition, the maximum peaks (400), (222) and (440) appear prominently, indicating the coexistence of <100>, <111> and <110> textures. At 200 °C, both (222) and (400) peaks decrease and at 300 °C, the (222) peak increases slowly and the (400) peak becomes very strong, resulting in a preferred orientation in the <100> direction, which is correlated with a decrease of the donor sites trapped at dislocations or point defects aggregates and the increase of the ITO films conductivity [26].

The ratio between the intensity of (222) peak to (400) peak (I_{222}/I_{400}) for the films annealed at 300 °C is 0.42 (see table 1) which is much less than the standard value for ITO powder [22].

Therefore the most part of the layer parallel to surface has been textured in <100> direction, while for films annealed at 400 °C this ratio is near standard value, resulting in the <111> textured films (table 1). In this case, annealing at 400 °C, ITO layers have more reduced oxygen vacancies and tend to grow in (222) direction so the resistivity of films increases. At 500 °C, (400) peak is a bit stronger than (222) peak, now that conductivity of the layer decreases.

The lattice constant (calculated from XRD strongest peak) and interplaner distances (d) of the film are summarized in table 1. It can be realized that the as-grown films are under tensile stress [27]. The larger value of lattice constant can fairly be attributed to the introduction of Sn atom into the crystal lattice.

None of the spectra indicated any characteristic peaks of Sn, SnO and/or SnO_2, which means that the tin atoms were probably doped substitutionally into the In_2O_3 lattice. The lattice constant and plane distances decrease by increasing annealing temperature. This can be related to higher oxygen vacancies at higher annealing temperature.

The evolution of the optical and electrical characteristics with increasing annealing temperature in vacuum is illustrated in Figs. 3 and 4 for ITO samples.

The resistivity of ITO films drastically decreases with increase in the annealing temperature and reached to $\approx1\times10^{-4}$ Ωcm and then to 7.3×10^{-5} Ωcm in 400 and 500 °C, respectively.

Fig. 4 shows that by increasing the annealing temperature average transmittance in visible region decreases. It can be related to increasing the carrier concentration in higher temperatures. The calculated average transmissions (T_{avr}) in the visible region of spectrum and resistivity given in table 1, shows that these two are opposite of each other.

In the region of the longer wavelengths the optical transmittance decreases for higher annealing temperature, resulting from a higher concentration of free carriers that also gives lower resistivity values.

It can be seen in Fig. 5 for typical as-deposited and annealed at 500 °C ITO layers. This can be related to improvements in the crystallinity, leading to a decrease of donor sites trapped at the dislocations and grain boundaries, and also to the out-diffusion of oxygen atoms from interstitial positions.

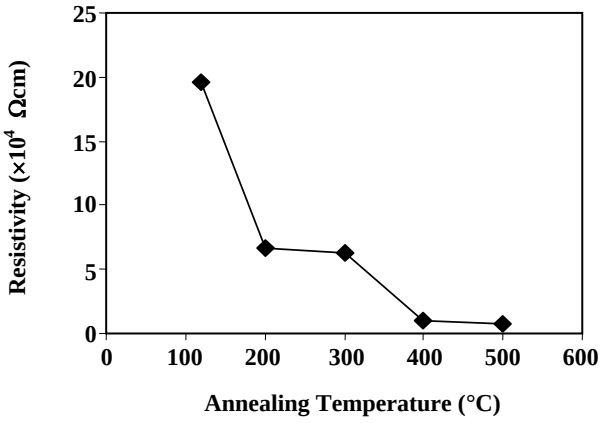

Fig. 3: Resistivity of the ITO films deposited and annealed at different annealing temperature in vacuum.

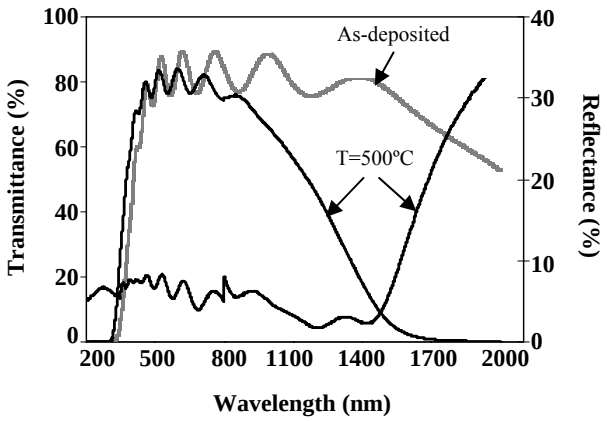

Fig. 5: Typically optical transmittance of ITO coatings on glass: as-deposited, annealed at 500 °C.

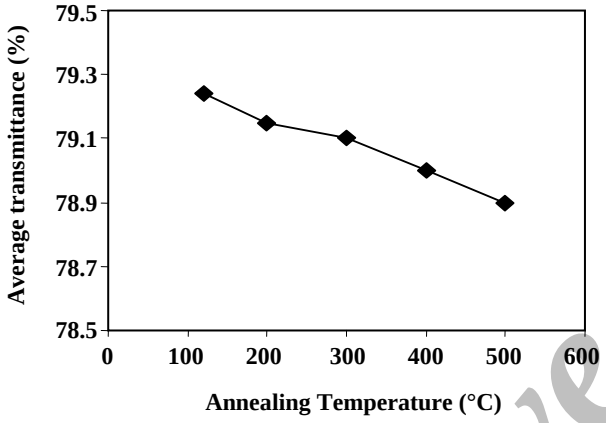

Fig. 4: Average Transmittance in visible region of the ITO layers as function of Annealing Temperature.

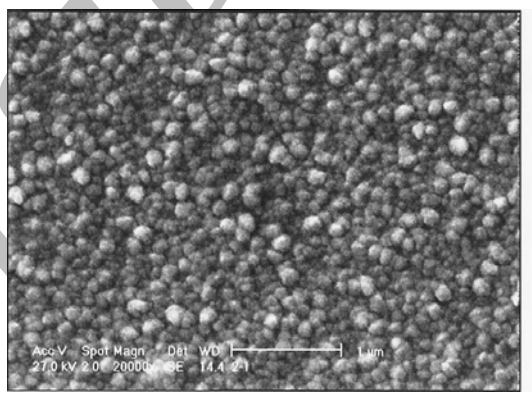

Fig. 6: SEM surface topograph of ITO film annealed at 500 °C.

The optical absorption coefficient (α) was calculated from the transmittance spectra and also energy gap (E_g) of films was determined using α^2 versus hυ plot [27]. The decrease in energy gap for the films annealed in different temperatures can be attributed to increasing oxygen vacancy. This is well supported by film's resistivity variation (table 1).

On annealing in vacuum, there is no reaction of the free oxygen in air with the ITO films; just the crystalline structure of the films tends to become perfect. Some oxygen atoms absorbed at surface escape and it causes the increase of the carrier concentration, consequently, the resistivity of the ITO films decreases.

Fig. 6 shows the surface morphology of ITO films deposited on glass and annealed at 500 ºC in vacuum furnace. It can be seen from the image that the film is dense, rather uniform and most of grains have a same size.

CONCLUSIONS

ITO films have been deposited on glass substrates using RF sputtering from ceramic target (In_2O_3-SnO_2, 90-10 wt. %) without extra heating. The post annealing was carried out from 200 °C to 500 °C in vacuum ambient.

The films crystal orientation changed from (100) to (111) as the annealing temperature increased to 400˚C and came back to (100) at 500 °C. By increasing the annealing temperature, average transmittance in visible region decreases. It can be related to increasing the carrier concentration in higher temperatures. SEM image of 500 °C annealed ITO thin film shows that the layer is rather uniform and a granular crystalline structure was formed. Results showed that the increase of the annealing temperature in vacuum improves the crystallinity of the films and also improves the electrical properties as well as the optical properties.

The resistivity of the deposited film is 19×10^{-4} Ωcm and falls down to 7.3×10^{-5} Ωcm as the annealing temperature increased to 500 °C in vacuum.

Acknowledgements

This project has been supported by Iran National Science Foundation (INSF).

Received : 28th November 2007 ; Accepted : 11th November 2008

REFERENCES

[1] Galasso, F.S., "Oxford, New York, Toronto, Sydney, Branschweing, Pergamon Press", **90** (1970).

[2] Elfallal, I., Rilkington, R. D., Hill, A. E., *Journal of Thin Solid Films,* **223**, 303 (1993).

[3] Ederth, J., Doctoral Degree Dissertation, Uppsala University, 4 (2003).

[4] Nadaud, N., Lequeux, N., Nanot, M., Jove, J., Roisnel, T., *Journal of Solid State Chem.*, **135**, 140 (1998).

[5] Yamada, N., Yasui, I., Shigesato, Y., Li, Y., Ujihira, Y., Nomura, K., *Jpn. J. Appl. Phys.*, **38(5A)**, 2856 (1999).

[6] Devi, P. S., Chatterjee, M., Ganguli, D., *Materials Letters*, **55**, 205 (2002).

[7] Nguyen, T.P., Le Rendu, P., Dinh, N.N., Fourmigue, M., Meziere, C., Young, G. O., *Synthetic Metals,* **138**, 229 (2003).

[8] Luff, B.J., Wilkinson, J.S., Perrone, G., *Appl. Optics*, **36**, 7066 (1997).

[9] Herrero, J., Guillen, C., *Vacuum,* **67**, 611 (2002).

[10] Teixeira, V., Cui, H. N., Meng, L. J., Fortunato, E., Martins, R., *Journal of Thin Solid Films,* **420-421**, 70 (2002).

[11] Kojima, M., Takahashi, F., Kinoshita, K., Nishibe, T., Ichidate, M., *Journal of Thin Solid Films,* **392**, 349 (2001).

[12] Fan, J. C. C., Bachner, F. J., Foley, G. H., *Journal of Applied Physics Letters,* **31(11)**, 773 (1977).

[13] Sreenivas, K., Sundarsena Rao, T., Mansnigh, A., Chandra, S., *Journal of Applied Physics,* **57(2)**, 384 (1985).

[14] Kim, H., Horwitz, J. S., Kim, W. H., Kafafi, Z., Chrisey, D. B., *Journal of Materials Research Society Symposium- Proceedings,* **780**, 21 (2003).

[15] Buchanan, M., Webb, J. B., Williams, D. F., *Journal of Thin Solid Films,* **80**, 373 (1981).

[16] Higuchi, M., Uekusa, S., Nakano, R., Yokogawa, K., *Japanese Journal of Applied Physics*, **33**, 302 (1994).

[17] Balasubramanian, N., Subrahmanyam, A., *Journal of Material Science and Engineering,* **B1**, 279 (1988).

[18] Bergman, J., Shapira, Y., Aharoni, H., *Journal of Applied Physics,* **67(8)**, 3750 (1990).

[19] Haitjema, H., Elich, J. J. Ph., *Journal of Thin Solid Films*, **205**, 93 (1991).

[20] Alam, M. J., Cameron, D. C., *Journal of Thin Solid Films*, **420-421**, 76 (2002).

[21] Jung, Y. S., *Journal of Solid State Commune,* **129**, 491 (2004).

[22] Guillen, C., Herrero, J., *Journal of Thin Solid Films,* **510**, 260 (2006).

[23] Hu, Y., Diao, X., Wang, C., Hao, W., Wang, T., *Journal of Vacuum*, **75**, 183 (2004).

[24] Daoudi, K., Canut, B., Blanchin, M.G., Sandu, C.S., Teodorescu, V.S., Roger, J.A., *Materials Science and Engineering C* **21**, 313 (2002).

[25] Mirzae, F., Maleki, M. H., Mirjalili, G., 14th Conference on Optics and Photonics Proceedings, (2008).

[26] Shigesato, Y., Paine, D. C., *Journal of Thin Solid Films*, **238**, 44 (1994).

[27] Kerkach, L., Layadi, A., Dogheche, E., Remiens, D., *J. Phys. D: Appl. Phys.*, **39**, 184 (2006).